

1

2

3 Title: **HIV-1 evasion of restriction factors: cyclophilin A and cell fusion provide a helping hand.**

4

5 Authors: Henry Owen*¹, Alun Vaughan-Jackson*¹, Lea Nussbaum¹, Jane Vowles¹, William
6 James¹, M.D.Moore^{1#}

7

8 *Authors contributed equally.

9 #Corresponding author. email: Kenny.moore@medsci.ox.ac.uk

10 Affiliations:

11 ¹Sir William Dunn School of Pathology, University of Oxford, South Parks Road, OX1 3RE

12

13 Running Title: Cellular assistance in HIV-1 evasion of restriction

14

15 Abstract word count: 168

16 Text word count: 5468

17

18

19 Abstract

20 Retroviral restriction factors are important regulators of viral infection, targeting vulnerable
21 steps of the virus lifecycle; steps that are also targeted by antiviral drugs. It has become clear
22 that the route of cellular infection can alter the sensitivity of HIV-1 to these agents. Using
23 CRISPR-Cas9 edited pluripotent stem cell-derived macrophages, we have explored the potential
24 of a modified restriction factor (human TRIMCyp) to inhibit HIV-1 replication in both cell free
25 and cell-cell infection models. We show that the expression of TRIMCyp from the endogenous
26 TRIM5 α locus potently restricts infection by cell-free HIV-1. Our results also show the
27 importance of the human cyclophilin A-HIV-1 capsid interaction for viral escape from restriction
28 by native human TRIM5 α , highlighting the evolutionary interplay between virus and this host
29 restriction factor. However, when co-cultured with infected T cells, stem cell-derived
30 macrophages are primarily infected by fusion between the cells. We have termed infected cells
31 that result from these fusions heterocytia, and show that their formation overcomes multiple
32 restriction factors and the reverse transcriptase inhibitor AZT.

33 Importance

34 As sentinels of the immune system, macrophages are relatively resistant to infection by
35 pathogens such as HIV-1. However, infected macrophages are found in infected patients and
36 they play key roles in the pathogenesis of the disease as well as being a component of the viral
37 reservoir that must be targeted before treatment can become cure. In this article, we show that
38 some of the mechanisms by which macrophages restrict HIV-1 can be overcome through a
39 recently described cell-cell interaction leading to cell-cell fusion. We also highlight an

40 evolutionary battle between virus and host and show how the virus has co-opted a host protein
41 to protect it from destruction by an antiviral mechanism. These two key findings suggest
42 potential novel treatment strategies that may reduce the viral reservoir and help our natural
43 defences take back control from the virus.

44

45 Introduction

46 Tissue resident macrophages are important for homeostasis, development and protection from
47 invading pathogens (1). Their role against pathogens includes detection of pathogen-associated
48 molecular patterns (PAMPs) by their numerous pattern recognition receptors (PRRs),
49 inactivation of the pathogen, innate signalling via interferon to bolster the defences of
50 surrounding cells, and antigen presentation to initiate an adaptive immune response. However,
51 being at the first line of defence also makes subversion of macrophages an evolutionarily
52 successful strategy for pathogens. As expressers of both CD4 and CCR5, macrophages stand
53 alongside T cells as a natural host cell for HIV-1, and as a self-renewing population of tissue
54 resident cells they also constitute a long-lived, inaccessible reservoir of virus that hampers viral
55 clearance strategies (2). Consistent with their immune role, macrophages have several antiviral
56 mechanisms to prevent infection by retroviruses such as HIV-1, namely the constitutive
57 expression of retroviral restriction factors, e.g. TRIM5 α and SAMHD1 (3).

58 TRIM5 α binds to the viral capsid lattice of an incoming, retroviral core and results in early
59 uncoating, proteasomal degradation of the viral capsid, and ultimately inhibition of reverse
60 transcription; however human TRIM5 α is inactive against HIV-1 (4). TRIM5 α can be saturated

61 by large doses of virus e.g. during viral dissemination via virological synapses, and can also be
62 circumvented by alterations in the viral capsid gene that prevent TRIM5 α binding (5, 6). The
63 compatibility between the viral capsid sequence and the host species TRIM5 locus is a major
64 determinant of successful infection. In fact, converting a single amino acid to the equivalent in
65 rhesus macaque TRIM5 α is sufficient to enable human TRIM5 α to restrict HIV-1 (7). The same
66 region of capsid that determines the sensitivity of HIV-1 to TRIM5 α is also the binding site for
67 the host peptidyl prolyl isomerase enzyme cyclophilin A (CypA) (8). Binding of CypA to an
68 incoming HIV-1 capsid prevents detection of reverse transcription products by macrophages,
69 and the subsequent production of IFN, but conversely binding of CypA aids restriction by TRIM5
70 of some monkey species (9). This interaction site has been the focus of an evolutionary arms
71 race between the TRIM5 locus and the simian relatives of HIV-1. In several monkey species
72 (e.g. Rhesus macaques and Owl monkeys) multiple retrotransposition events resulted in CypA
73 being inserted into the TRIM5 locus, producing a novel antiviral protein, TRIMCyp (10, 11).
74 Although TRIMCyp does not contain the usual PRYSPRY domain for viral binding, it uses the
75 CypA domain to bind the capsid of sensitive viruses. The species-specific activity of TRIM5 and
76 TRIMCyp suggest that they act as cross-species barriers to retrovirus infection (12, 13), and that
77 in consequence, the TRIM5 locus has great potential to act as a target for gene therapy. To that
78 end, it has been shown that overexpression of macaque TRIM5 variants or TRIMCyp in human
79 cells results in protection from HIV-1 infection (14, 15). However, these approaches fail to take
80 account of the role of endogenous TRIM5 α as both a target and signaller of the IFN system (16),
81 nor any potentially adverse consequences of overexpression of this potent antiviral element.

82 The other major restriction factor expressed by macrophages, SAMHD1, is a deoxynucleotide
83 triphosphohydrolase enzyme (17). The activity of SAMHD1, conversion of dNTPs into
84 deoxynucleosides (dNs), is essential to maintain balanced levels of dNTPs within cells, which is
85 required for genome stability in dividing cells, and is used to reduce the availability of dNTPs to
86 invading pathogens such as HIV and *Leishmania* in non-dividing cells (18-20). In activated T
87 cells, SAMHD1 is both expressed poorly and inactivated by phosphorylation, thus it is unable to
88 inhibit HIV-1 infection (21-23). In contrast, in terminally differentiated macrophages, SAMHD1
89 is expressed at high levels, is dephosphorylated, and reduces the levels of dNTPs to below the
90 level required by the viral RT enzyme for efficient reverse transcription (19). Although HIV-1
91 has evolved to be able to replicate, albeit inefficiently, under these conditions, the virus has not
92 evolved a specific counter measure such as VPx of SIV and HIV-2 that targets SAMHD1 for
93 degradation (24), implying that HIV-1 infection is macrophage independent or that the virus has
94 evolved a novel way of bypassing this restriction.

95 In this report, we use CRISPR/Cas9 to alter the restriction factors TRIM5 α and SAMHD1 in order
96 to investigate their impact on the infection of macrophages by HIV-1. By investigating both cell-
97 free and cell-associated infection models we confirm the potency of these factors, but also
98 highlight cell fusion as a mechanism by which they can both be efficiently overcome within
99 tissue macrophages. For this work, we used pluripotent stem cell-derived macrophages (pMac)
100 as a model system for tissue macrophages, as they are genetically tractable at the stem cell
101 stage, karyotypically normal and terminally differentiated, as well as being ontologically,
102 phenotypically and transcriptomically similar to authentic tissue macrophages (25, 26), features
103 not associated with cancerous cell lines or blood monocyte-derived macrophages.

104 Results

105 Endogenous human TRIMCyp Inhibits HIV-1 Infection

106 To measure the impact of TRIMCyp in human cells expressed at levels comparable with
107 endogenous TRIM5 α , we generated a pluripotent stem cell line containing a knock-in of human
108 CypA into exon 8 of TRIM5 α using a double nicking CRISPR-Cas9 approach (Fig 1A) (27). A single
109 clone was identified carrying the CypA insertion in both alleles of TRIM5, as demonstrated by
110 the single peaks of the sequencing trace (Fig 1B) that correspond to the fusion of TRIM5 with
111 CypA at Serine 322 of TRIM5 (28). To observe the effect of human TRIMCyp on HIV-1 infection,
112 the pluripotent stem cells and their differentiated macrophage progeny (pMac) (29) were
113 exposed to increasing doses of a single-cycle GFP-expressing reporter virus, pseudotyped with
114 VSV-G.

115 Infectivity in both stem cells and pMacs was reduced by conversion of TRIM5 α to TRIMCyp (Fig
116 1C+D, and FigS1A+S2A). As TRIMCyp is inserted into the TRIM5 locus it can be considered a
117 marker of TRIM5 expression in wild-type cells, thus reduced infectivity of gene-edited stem cells
118 indicates that TRIM5 α is normally expressed in pluripotent stem cells, potentially as a
119 mechanism to prevent endogenous and exogenous retroviral infections of the embryo (30). In
120 pMacs, TRIMCyp has a more dramatic impact on infectivity than in stem cells, reducing
121 infection by 10-fold at most viral concentrations (Fig S2A). At higher concentrations of virus
122 (shown in Fig S2A) it is possible to observe the well-established saturation of TRIM-based
123 restriction, such as rhesus TRIM5 α and owl monkey TRIMCyp (31). To demonstrate that the
124 reduction in infection, seen in Fig 1C+D and Fig S1A+2A, was due to the modification at the

125 TRIM5 α locus and not to any off-target effect, the cells were treated with CsA during infection.
126 CsA prevents CypA from binding the viral capsid and is known to rescue HIV-1 infection in
127 TRIMCyp expressing cells. CsA has also been shown to reduce HIV-1 infectivity in human cells by
128 an incompletely understood mechanism that has been linked to HIV-1 genome detection by
129 cellular DNA detection pathways (9). In agreement with these data, our wild-type cells were
130 more resistant to infection after treatment with CsA (Fig 1C+D, Fig S1B+S2B), whereas
131 treatment of the gene edited stem cells and pMacs with CsA significantly inhibited restriction of
132 HIV-1 by TRIMCyp (Fig 1C+D, Fig S1C+S2C).

133 Human cyclophilin A protects HIV-1 from human TRIM5 α

134 Other than overall size of effect, a major difference that is observed between the pluripotent
135 stem cell progenitors and the differentiated pMacs, is a disparity between the unmodified and
136 modified cells when both are treated with CsA (Fig 1C+D). If one compares the results of wild-
137 type macrophages expressing human TRIM5 α with those of CsA-treated TRIMCyp-expressing
138 cells (which express CsA-inactivated TRIMCyp, but no human TRIM5 α) it would appear that
139 TRIM5 α has little or no activity against HIV-1 (Fig S1D+S2D), confirming previously published
140 data (32). However, the comparison of HIV-1-infection in the isogenic TRIM5 α and TRIMCyp
141 macrophages both in the presence of CsA, reveals a residual antiviral effect of TRIM5 α . If
142 human TRIM5 α did not bind HIV-1, and CsA prevented TRIMCyp from binding, then in the
143 presence of CsA both cells should have the same infectivity to HIV-1. However, as can be seen
144 in Fig 1D and Fig S2E, TRIM5 α -expressing pMacs treated with CsA are more resistant to HIV-1
145 than CsA-treated TRIMCyp-expressing pMacs, suggesting an interaction of human TRIM5 α with
146 the viral core when CypA binding is prevented. We hypothesise that HIV-1 has evolved to use

147 CypA, to alter its conformation, as an evasion strategy to escape TRIM5 α restriction. However,
148 as stem cells did not show this phenotype (Fig 1C and Fig S1E) the impact of TRIM5 α on CypA-
149 deficient viruses appears to be cell-type dependent, as has recently been shown for TRIM5 α
150 function in Langerhans cells (33), possibly due to reduced effectiveness of downstream
151 effectors in stem cells (34).

152 As the infection results were obtained using an exogenous reporter (eGFP) virus pseudotyped
153 with VSV-G, an envelope that has been previously been shown to alter susceptibility to TRIM5 α
154 restriction (33), we performed the same infection experiments in pMacs using three different
155 vectors that were pseudotyped with JRFL, a cognate macrophage-tropic HIV-1 envelope
156 protein. As the different vectors had different reporter genes (eGFP or luciferase) the results
157 were normalized to the infectivity of wild-type TRIM5 α expressing cells. The results confirm
158 those of the VSV-G pseudotyped vectors, with a 10-fold reduction in infectivity in both CsA-
159 treated wild-type cells and in TRIMCyp-expressing cells, but a recovery of infection with CsA
160 treatment of TRIMCyp-expressing cells over that of CsA-treated wild-type cells (Fig 1E).

161 To observe the impact of TRIMCyp in a more physiological setting, pMacs were exposed to wild-
162 type replication-competent HIV-1 with a luciferase reporter expressed in the Nef open reading
163 frame (NL-LucR.T2A). Tracking the infection over a 5-day period shows a robust growth of HIV-1
164 in TRIM5 α -expressing cells, but not in TRIMCyp-expressing cells (Fig 1F, inset). Although CsA
165 could inhibit replication in TRIM5 α -expressing cells, it was not able to significantly alter
166 infectivity of TRIMCyp expressing cells (Fig 1F), possibly due to the multifaceted way CypA is
167 employed by the virus and, therefore, multiple stages of the virus lifecycle that could be
168 affected by CsA (16, 35).

169 To directly investigate the hypothesis that CypA alters the susceptibility of HIV-1 to human
170 TRIM5 α restriction, we generated pMacs knocked out for human TRIM5 α using CRISPR/Cas9
171 (Fig 1A). Exposure of these cells to an HIV-1-based vector clearly confirms previous data
172 showing a lack of robust restriction of HIV-1 by endogenous human TRIM5 α (Fig 1G). However,
173 in the presence of CsA the loss of infectivity observed with wild-type cells is abrogated by
174 removal of TRIM5 α (Fig 1G), which genetically proves our hypothesis (Fig S2F). To confirm the
175 role of CypA in protection of HIV-1 from TRIM5 α , the cells were exposed to the same reporter
176 vector but harbouring the P90A mutation in capsid that prevents CypA binding. In line with the
177 published literature, the P90A mutant is not affected by cell treatment with CsA, but in
178 agreement with our hypothesis, the P90A mutant is more infectious in TRIM5 α -knockout pMacs
179 compared with wild-type cells (Fig 1H).

180

181 TRIMCyp is circumvented by cell fusion

182 As TRIM5 α and TRIMCyp restriction can be overcome by saturation with incoming viral cores
183 (31), and it is known that cell-to-cell transmission (e.g. via a virological synapse) can result in
184 large quantities of viral material being transferred to the target cell (36, 37), we set out to
185 establish whether endogenous levels of TRIMCyp were sufficient to protect cells in the more
186 physiological setting of cell-cell contact. To test this, we employed the same experimental set
187 up that was used to demonstrate phagocytosis of infected T cells as a potential route for HIV-1
188 infection of macrophages (38), with some minor adjustments. As an initial experiment, NL-
189 LucR.T2A infected Jurkat-R5 cells were co-cultured with wild-type or TRIMCyp macrophages for

190 6 hours and infection of the macrophages was assessed 7 days later (Fig 2A). In contrast to the
191 data obtained by Baxter et al. 2014, we did not see a significant difference between infection
192 levels in the presence or absence of the reverse transcriptase inhibitor AZT, even though in
193 experiments using cell-free virus, AZT reduced infection of the macrophages (Fig 2B). To
194 investigate the reverse transcriptase-independent results further, and to show that the results
195 were not dependent on the genotype of the induced pluripotent stem cell donor, the
196 experiment was repeated using pMacs from three independent donors, using both AZT and the
197 fusion inhibitor, T20 or enfuvirtide (39). Once again, the level of infection was unaffected by
198 AZT, however T20 reduced the level of infection more than 10-fold (Fig 2C), indicating that HIV-
199 1 envelope-driven fusion of the cells was the major cause of the observed infection, a process
200 that appears to be unaffected by TRIMCyp expression.

201 To test the hypothesis that T cell-macrophage fusion bypasses TRIM-based restriction in a more
202 physiological setting, PBMC-derived CD4+ T cells from three independent donors were infected
203 with NL-LucR.T2A and co-cultured with wild-type or TRIMCyp-expressing pMacs in the presence
204 of AZT, T20 and the IFN-signalling inhibitor Ruxolitinib (Rux). Again, the levels of infection were
205 not significantly altered by the presence of AZT, whereas T20 significantly reduced infection (Fig
206 2D). Additionally, preventing IFN signalling enhanced infection, particularly in the TRIM5 α
207 expressing cells (Fig 2D). By subtracting the background signal of fusion-induced infection (AZT
208 control), it is possible to observe replication of HIV-1 during and/or after the co-culture (Fig 2E),
209 which highlights the significant impact of TRIMCyp expression as well as IFN in this
210 experimental setting. A Luminex[®] assay on the culture supernatants confirmed the release of
211 IFN α in untreated conditions and an elevation of the proinflammatory cytokine IL-1 β , without

212 any impact on the other cytokines/chemokines assayed, e.g. the chemoattractant MCP-1 (Fig
213 2F).

214 Upon observing the co-cultures of macrophages and PBMC-derived T cells by light microscopy it
215 became apparent that a major difference between the treatments was the absence of giant
216 syncytial cells in the T20 treated cells (Fig. 2G). It has been known for many years that HIV-1-
217 directed fusion between macrophages can result in giant multinucleated syncytia (40, 41).
218 However, given that the majority of infection in the macrophages was independent of HIV-1
219 reverse transcription (AZT result in Fig. 2A+D), we hypothesised that the major route of
220 macrophage infection in our experimental setting was T cell-macrophage fusion. To address
221 this, we performed live cell fluorescence microscopy on co-cultures of CellTracker™ Orange
222 CMRA-stained pMacs with T cells infected by an eGFP-expressing replication-competent HIV-1.
223 Within 30 minutes, fusion between T cells and macrophages was observed in the co-cultures,
224 with the eGFP-tagged HIV-1 Gag protein being rapidly transferred from the T cell to the
225 macrophage over a period of 5 minutes (Fig 3A and Video S1). This process resulted in
226 macrophages harbouring an infected T cell-derived nucleus in the absence of reverse
227 transcription. The destiny of each virally infected T cell was quantified over a 2-hour period
228 post-co-culture (Fig 3B). The major events included both cell-cell fusion (rapid mixing of the
229 cytoplasmic contents) and cell capture (attachment and colocalisation of a T cell within a
230 macrophage, without cytoplasmic mixing, in a process consistent with phagocytosis of live cells,
231 in Fig S3A, or apoptotic cells in Fig S3B (38)). Additional events included rapid loss of GFP signal
232 from the T cell in a process consistent with cell lysis (Fig S3C) and transfer of virus from the T
233 cell to the macrophage in a process consistent with the formation of a virological synapse or

234 plasma membrane transfer between immune cells (Fig S3D) (42, 43). The only event that was
235 modified by antiviral drug treatment was cell fusion by T20, demonstrating that the results for
236 cell-cell infection (Fig 2A+C+D) were the outcome of the formation of a fusion of infected T cells
237 with uninfected macrophages; the product of which we have termed heterocytia, to distinguish
238 them from syncytia, derived from a single cell type, and heterokaryons, derived from
239 genetically different parents.

240 Heterocytia formation overcomes SAMHD1 restriction

241 Given the ability of heterocytia formation to overcome potent TRIMCyp restriction and to result
242 in infected macrophages without reverse transcription, we next investigated if the other major
243 antiretroviral mechanism employed by macrophages, SAMHD1, was also circumvented. We
244 have previously generated macrophages from pluripotent stem cells genetically ablated for the
245 retroviral restriction factor SAMHD1 (44). SAMHD1 knockout macrophages show faster and
246 more efficient infection by HIV-1 when exposed to NL-LucR.T2A virions (Fig 3C). However,
247 when cocultured with NL-LucR.T2A -infected T cells, the isogenic pairs of macrophages,
248 differing only by the presence of SAMHD1, show similar levels of infection (Fig 3D). This
249 infection is unaffected by AZT, but reduced by T20, which demonstrates that cell fusion not only
250 bypasses TRIM5 α -mediated restriction but also SAMHD1 restriction, making it independent of
251 the major retroviral restriction factors and, therefore, potentially the most efficient method of
252 macrophage infection.

253 Given that in dividing cells SAMHD1 is inactivated by cyclin dependent kinase (CDK)
254 phosphorylation at T592 we hypothesized that cell fusion would also alter the regulation of

255 pMac SAMHD1. Within macrophages, SAMHD1 is generally unphosphorylated, and therefore
256 active, whereas in T cell lines such as CEM cells it is not expressed. Therefore, upon fusion
257 between the two cells, any detected increase in phosphorylated SAMHD1 would indicate an
258 interaction between the cells' proteomes. We co-cultured pMacs from three donors with a CEM
259 cell line constitutively expressing the HIV envelope, for 24 hours before lysing the cells and
260 probing for SAMHD1 phosphorylation by western blot. Quantification of the ratio of
261 phosphorylated SAMHD1 to total SAMHD1 shows that the pMac SAMHD1 is inactivated by
262 fusion with the T cell (Fig 3E and Fig S4E).

263 Heterocytia formation occurs in stem cell-derived microglia

264 To investigate the potential of T cells to fuse with microglia in the brain and thereby generate
265 giant cells, frequently observed in HIV encephalopathy, we employed our recently described
266 and validated pluripotent stem cell model of microglia (26). Differentiating stem cell-derived
267 macrophages in the presence of IL-34 results in microglial progenitor like cells (pMGL) that
268 adopt highly ramified and mobile phenotypes characteristic of microglia in vivo. Addition of T
269 cells infected with an eGFP-expressing replication competent reporter virus to tRFP-expressing
270 pMGLs resulted in not only the heterocytia observed with pMacs, but also giant multinucleated
271 cells with peripherally arranged nuclei that more closely resemble tissue giant cells, e.g.
272 Langhans giant cells, HIV-associated giant cells of the lymphoid Waldeyer's ring, and HIV
273 encephalitis associated multinucleated cells (Fig 3F) (40, 41).

274

275 Discussion

276 Macrophages are inherently resistant to HIV-1 infection due to low levels of the viral receptors
277 CD4 and CCR5, high levels of active SAMHD1, and the ability to detect and respond to infections
278 with a robust innate response. Nevertheless, they represent a natural target cell for HIV-1 *in*
279 *vivo*, contributing to the viral reservoir (45), and are perhaps the most elusive targets for drug
280 treatment, residing in difficult to reach regions such as the CNS, in the form of microglia (46).
281 Most studies into HIV-1 infection of macrophages make use of either monocytic cell lines that
282 have altered cell cycle control and loss of SAMHD1 activity, or blood monocyte-derived
283 macrophages differentiated *in vitro* under various non-physiological conditions, e.g. high levels
284 of FCS, which is known to alter SAMHD1 activity (47). Given the importance of SAMHD1 in
285 repressing HIV-1 replication, neither of these cellular models is ideal. Moreover, in most tissues
286 monocytes only invade and differentiate into macrophages under inflammatory conditions, so
287 their role in HIV-1 transmission and subsequent pathogenesis is unclear. In contrast, tissue
288 resident macrophages are present within all tissues at steady state, including within the mucosa
289 at the site of infection and, in most tissues, are ontologically distinct from monocytes, being
290 derived from Myb-independent erythro-myeloid progenitors (EMP) of the yolk sac and foetal
291 liver during embryogenesis, not hematopoietic stem cells of the adult bone marrow (2). We
292 have recently shown that pluripotent stem cell-derived macrophages differentiate via an EMP,
293 in a Myb-independent manner (25). Thus, we feel that they are an excellent model of tissue
294 resident macrophages such as microglia, and could help to define the molecular and cellular
295 players during transmission at the mucosa and during neuropathology.

296 In this work we have used the stem cell-derived model of tissue macrophages to explore the
297 role of TRIM5 α on HIV-1 infection. Through genetic manipulation of the human TRIM5 α locus to

298 encode the anti-HIV-1 restriction factor TRIMCyp, we have shown that endogenous levels of
299 this protein provide the cells with potent protection from HIV-1 replication. Using CsA to
300 prevent the activity of the CypA component of TRIMCyp, we have also revealed an interesting
301 feature of native human TRIM5 α activity. It has long been established that human TRIM5 α has
302 little to no activity against HIV-1, however there has been confusion over the impact of CsA on
303 this activity. Initial work suggested that CsA was able to enhance the activity of TRIM5 α (48),
304 however the same group and others subsequently presented data that conflicted with this
305 concept (49-51). The current model of CsA action involves destabilization of the viral capsid
306 through loss of CypA binding, resulting in early detection of nascent HIV-1 DNA by cGAS, IFN α
307 production, and suboptimal integration site selection (52). The genetic data presented here
308 shows that TRIM5 α does inhibit HIV-1 under conditions in which viral cores lack CypA, either
309 through treatment with CsA or the P90A mutation of Gag. As TRIM5 α has been shown to
310 destabilize cores in susceptible virions (53), we hypothesize that without CypA, TRIM5 α binds
311 the core, reducing its stability and resulting in detection of the viral DNA. This suggests that
312 HIV-1 evolved to bind CypA as a direct countermeasure to the activity of human TRIM5 α , with
313 the added benefit of keeping the virus from detection by the innate immune response. This
314 would suggest that CsA, or one of its non-immunosuppressive variants (54, 55), could be used
315 therapeutically to assist the antiviral effects of endogenous TRIM5 α . However, previous
316 attempts using CsA in HIV-1 patients have met with mixed success (56-58). Moreover, as we
317 have identified heterocytium-formation as a potentially significant cell-cell infection pathway,
318 even this approach to activate TRIM5 α could be circumvented.

319

320 Although infection by cell-free HIV-1 can occur, cell-cell interactions have been shown to
321 enhance transmission between cells. The virological synapse (43), tunnelling nanotubes (59)
322 and phagocytosis of infected T cells (38) have all been observed to enable directed transmission
323 of HIV-1 between cells. However, these all require reverse transcription, a weak link in the viral
324 lifecycle that is targeted by multiple restriction factors (e.g. APOBEC3G/F, SAMHD1, TRIM5) and
325 is a key drug target (e.g. NNRTIs and NRTIs). The data presented here show that cell fusion
326 between T cells and macrophages is an efficient infection process, resulting in an infected
327 heterocytium, that bypasses reverse transcription, thereby avoiding reverse transcription-
328 targeting restriction factors and antiviral drugs.

329 Syncytium-formation is a fundamental property of mammalian development, being at the heart
330 of trophoblast formation, osteoclast differentiation and muscle fiber generation. However,
331 syncytia are also found in many pathological settings, e.g. Langhans giant cells, giant cells of
332 granulomas and multinucleated giant cells of viral infection. From the perspective of HIV-1
333 infection, syncytium formation of *in vitro*-infected T cells has historically been linked to CXCR4-
334 tropic viral strains that are also associated with more rapid disease progression (60).

335 Heterocytia have also been observed within *ex vivo* cultured T cell and dendritic cell co-cultures
336 from tonsil lymph nodes from infected individuals (61). In vivo evidence for the existence of
337 syncytia was for a long time limited to immunohistochemical identification of multinucleated
338 giant cells within the CNS of HIV-associated encephalitis cases (62). More recent studies using
339 humanized mouse models have highlighted a significant amount of small T cell-derived syncytia
340 within the tight confines of lymphoid tissues (63). However, to date these HIV-1-induced
341 syncytia have been reported solely from a phenomenological viewpoint, with little research

342 into their pathophysiological consequences. HIV-1-driven T cell-macrophage fusion has also
343 been previously observed (64, 65), but as low frequency events under certain differentiation
344 conditions that promote the fusogenic properties of macrophages. Our data corroborate this
345 phenomenon and show that it is highly efficient in stem cell-derived macrophages, an authentic
346 cell model of tissue resident macrophages. Such fusion events, *in vivo*, between short-lived
347 infected T cells and long-lived self-renewing tissue macrophages could be of paramount
348 importance in establishing (1) a beachhead at the site of infection, and (2) a viral reservoir in
349 tissues such as the brain as infected T cells transit through the CNS and interact with microglia
350 (66). Additionally, during cross-species transmission events such interspecies heterocytia
351 would allow viral infections to overcome incompatibilities between the virus and innate
352 restriction factors, e.g. TRIM5 α . The presence of heterocytia *in vivo* would also provide an
353 alternative explanation for the observation of rearranged TCR DNA within macrophage
354 populations isolated from experimentally infected SIV rhesus macaques (67). Finally, although
355 this study does not address the pathophysiology of these heterocytia during HIV-1 infection,
356 the efficiency of their formation *in vitro* shown in this study, added to *in vivo* observations of
357 syncytia, suggests that they might be a valuable target for treatment. Given that our data
358 demonstrate that the formation of syncytia could be inhibited by the fusion inhibitor T20 and
359 could potentially be limited by IFN α , it is possible that early treatment with these antiviral
360 agents could prevent the neuropathological consequences of infection and reduce the
361 macrophage viral reservoir.

362

363 Materials and Methods

364 Cell Culture

365 Cell culture reagents were sourced from Invitrogen unless otherwise stated. Wild-type human
366 induced pluripotent cell lines SFC840-03-03 (26), SFC856-03-04 (26), OX1-19 (29) and AH016-3
367 Lenti_IP_RFP (26) and pluripotent stem cell line (HUES2) and its derivatives, have been
368 characterised previously (44). The induced pluripotent stem cell lines were originally derived
369 from healthy donors recruited through the Oxford Parkinson's Disease Centre having given
370 signed informed consent (Ethics Committee that specifically approved this part of the study,
371 National Health Service, Health Research Authority, NRES Committee South Central, Berkshire,
372 UK, REC 10/H0505/71). All experiments were performed in accordance with UK guidelines and
373 regulations and as set out in the REC. Stem cells were grown in mTeSRTM1 on Matrigel[®] (Corning)-
374 coated tissue culture dishes, passaged using TrypLETM and plated with the Rho-kinase inhibitor Y-
375 27632 (10 μ M; Abcam). Stem cells were differentiated into pMacs using an established
376 macrophage protocol(29), and where necessary were cultured in microglia induction media as
377 previously described (26). The CCR5-expressing T cell line, Jurkat-R5, was a kind gift from Prof. Q.
378 Sattentau. The HIV-1 envelope-expressing CEM T cell line (CEM-HO-BaL) was engineered using a
379 VSV-G-pseudotyped lentiviral vector co-expressing puromycin and HIV-1 BaL envelope, and a
380 second generation vector (NL4.3R⁺E⁻HSA-T2A-Nef) to provide all accessory proteins required for
381 BaL expression. Primary CD4 positive T cells were isolated from donor-derived peripheral blood
382 mononuclear cells (obtained with written informed consent) using the MACS (Miltenyi) CD4+ T
383 cell isolation kit according to the manufactures guidelines and were maintained in RPMI with 10%
384 foetal calf serum and 1% pen/strep and activated using 1 μ g/ml PMA and 10 units/ml IL-2 for 24
385 hrs, 3 days prior to infection with replication competent virus.

386 Genome Engineering

387 TRIMCyp modification: The CRISPR-Cas9 plasmids used in this study were based on the dual guide
388 RNA (gRNA) and Cas9^{D10A}-expressing plasmid, pX335-U6-Chimeric_BB-CBh-hSpCas9 (pX335), and
389 its puromycin-resistance gene-expressing derivative, pX462(68) (gifts from Feng Zhang; Addgene
390 plasmids #42335 and #48141). Cloning was performed as previous described(68) using
391 oligonucleotides TRIM1f (CACCGCGAAACCACACGATAATATAT) and TRIM1r
392 (AAACATATATTATCTGTGGTTTCGC) with BbsI digested pX335 to create pX335-Trim51,
393 oligonucleotides TRIM3f (CACCGACAGCACATGAAATGTTGTT) and TRIM3r
394 (AAACAACAACATTTTCATGTGCTGTC) with pX462 to create pX462-TRIM3. The donor template was
395 constructed from OX1.19 stem cell cDNA, amplifying three fragments: (1) the 5' homology arm
396 with primer TRIMcyp1f (TGGTACCGAGCTCGGATCCATGTCAAACACCCAGGAGC) and TRIMcyp1r
397 (TGGGGTTGACAGAGCTCACTTGTCTCTTATCTTC), (2) Cyclophilin A with primer TRIMcyp2f
398 (AGTGAGCTCTGTCAACCCACCGTGTC) and TRIMcyp2r
399 (GAGCCCAGGATTATTCGAGTTGTCCACAGTC) and (3) the 3' homologous arm with primer
400 TRIMcyp3f (ACTCGAATAATCCTGGGCTCTCAAAGTATC) and TRIMcyp3r
401 (TGGGCCCTCTAGATGCATGCACACTGCTGGTATATGGAGAG). The three fragments were
402 assembled using the Gibson Assembly® mastermix (NEB), according to the manufacturer's
403 guidelines, into XhoI and SpeI digested pCR2.1-TOPO (Invitrogen), to generate pTOPO-TRIMCyp.
404 The pluripotent stem cell line, SFC840-03-03, was Neon® (Invitrogen) transfected with pX335-
405 TRIM1, pX462-TRIM3 and pTOPO-TRIMCyp, as previously (69). Twenty-four hours post-
406 transfection cell were selected for 48 hours in 0.25 µg/ml puromycin. Once recovered the
407 surviving cells were plated on mouse embryonic fibroblasts and single cell cloned, as previously

408 (69). The correct genotype was identified by amplification of the TRIMCyp gene with primers
409 CypAF (CATTGCTGACTGTGGACAACTC) and OutR2 (GCCATTTAAGTATGTTATTCACAG), and was
410 shown to be a homozygous knock-in using primers TRIMsurF (CTGACAGATGTCCGACGCTACT) and
411 TRIMsurR (CGATCAGGACAAATAATCACAGAGA), the product of which was Sanger sequenced
412 using primer TRIMHRMr2 (ACACGTCTACCTCCCAGTAATGTTT)

413 TRIM5 Knockout: To knockout TRIM5 expression a lentiviral vector (pLentiCRISPRv2.0, gift from
414 Feng Zhang, Addgene plasmid # 52961) was used. Oligos targeting exon 2 of TRIM5 α
415 (CACCGTTGATCATTGTGCACGCCA and AAAGTGGCGTGACAATGATCAAC)

416 were annealed, phosphorylated and ligated into BsmBI digested vector as described (70). VSV-G
417 pseudotyped vector was used to transduce SFC840-03-03 cells, which were subsequently
418 selected with 1 μ g/ml puromycin for 7 days before single cell cloning on mouse embryonic
419 fibroblasts. Successful knockout clones were identified by Sanger sequencing of the PCR product
420 using primers TRIM5seqF (GTGAAAGCCCTGAGGCATAA) and TRIM5seqR
421 (CCTGCTGAAAGGGGTAATCA) followed by TIDE analysis (71). The two knockout clones used in
422 this work were a homozygous out-of-frame mutant (11 base pair deletion and single base pair
423 insertion) and a heterozygous double out-of-frame mutant (5 base pair deletion in one allele and
424 4 base pair deletion in the other).

425 Lentiviral transduction and Transfection

426 Lentiviral vectors were generated by PEI-mediated transient transfection of 293T cells using
427 pCMVdeltaR8.2 packaging vector for self-inactivating vectors and either pMD2.G for VSV-G
428 pseudotyped vectors (gifts from Didier Trono; Addgene plasmids #12263 and #12259), or pJRF1

429 for JRFL pseudotyped vectors. The vectors used included pHR'SIN-cPPT-PGK-GIP (a derivative of
430 pHR'SIN-cPPT-EF1-GIP (69)), pHIV-HIG (72), pNL4-3.Luc.R-E- (73, 74), pNL4.3R'E'eGFPT2ANef
431 (derived from pNL4-3.Luc.R-E- by replacing the luciferase gene with eGFP). Additionally, pNL4.3R'
432 E'eGFPT2ANef was modified to incorporate the capsid mutant, P90A, using annealed oligos
433 P90Afrd (CAGGGGCTATTGCACCAGGCCAGATGAGAGAACCAAGGGGAAGTGACATAGCAGGAACTA)
434 and P90Arev (CTAGTAGTTCCTGCTATGTCACTTCCCCTTGGTTCTCTCATCTGGCCTGGTGAATAGCCCCTGCATG).
435
436 To replace the fragment released by digestion with SphI and SpeI. Finally, pNL4.3R'E'eGFPT2ANef
437 was modified to include the selectable heat stable antigen (HSA) gene from pHIV-HIG. Where
438 required cells were pretreated with 5 μ M CsA or equivalent percentage of DMSO 2 hours prior
439 to infection with viral vectors. Stem cells and pMacs were plated 24 hours or 7 days, respectively,
440 prior to infection in 96 well plates in 100 μ l. Infection was carried out by replacing 50 μ l of
441 supernatant with 50 μ l of three-fold serial dilutions of virus and incubation for 3 days prior to
442 infectivity assay. Fluorescent viruses were quantified by flow cytometry (BD FACSCaliber) and
443 luciferase viruses were quantified by One-Glo™ Luciferase assay (Promega) according to
444 manufacturer's guidelines.

445 Replication Competent Assays

446 The BaL envelope-expressing replication competent viruses either with the reporter renilla
447 luciferase (NL-LucR.T2A (74)) or eGFP (NLENG1-BaL-eGFP, a derivative of NLENG1-IRES (75) with
448 the macrophage tropic BaL envelope) in the Nef reading frame, were generated by PEI
449 transfection of 293T cells. Viral infectivity was titred on TZM-bl cells and for infections of Jurkat-
450 R5 cells and primary CD4+ T cells an equivalent MOI of 0.05 was used. Infected Jurkat-R5 cells

451 were used 3 days post-infection whereas the primary CD4+ T cells were used 3-5 days post-
452 infection. For viral growth assays in pMacs the cells were infected at an MOI of 0.02 and the cells
453 were harvested in 24 hour periods and infectivity was quantified using Renilla-Glo[®] Luciferase
454 assay (Promega) according to the manufacturers protocol. For the cell-cell infectivity assay, NL-
455 LucR.T2A-infected T cells were added to day 7 differentiated pMacs at a ratio of 1:1, with or
456 without pre-treatment of pMacs with AZT (25 μ M), T20 (7.5 μ g/ml) or ruxolitinib (10 μ M). After
457 6 hours co-culture, the T cells were removed with a single wash in PBS followed by incubation of
458 the cells in macrophage differentiation media supplemented with 25 μ M etoposide for 7 days.

459 Cytokine release

460 Supernatant from day 7 co-cultures were assayed by Luminex using an 11-plex custom cytokine
461 panel (Affymetrix) according to the manufactures guidelines, except with the addition of a final
462 fixation with 2% paraformaldehyde for 30 mins at room temperature and two washes before
463 resuspension in reading buffer. Cytokines included IFN- α , IFN- β , IFN- γ , TNF- α , IL-10, IL-1 β , IL-6,
464 IL-8, IP-10, MCP-1 and RANTES.

465 Imaging of Co-cultures

466 Day seven differentiated pMacs were stained with 2 μ M CellTraker[™] Orange CMRA before
467 addition of Jurkat-R5 cells, infected 5 days previously with NLENG1-BaL-GFP, at a 2:1 ratio in
468 macrophage differentiation media with 1 μ g/ml Hoechst 33342. Cells were imaged on a Zeiss
469 Axiovert 200 microscope with Axiovision MRm camera and Colibri illumination every 5 minutes
470 for 2 hours. Images were processed with Axiovision software (Zeiss) and the fate of all GFP
471 labelled T cells across four fields of view per condition were quantified in a double blind manner.

472 Western Blot

473 CEM-H0-BaL or CEM-H0 T cells were added to 7 day differentiated pMacs at a 3:2 ratio for 16
474 hours in the presence or absence of 250 nM CCR5 antagonist Tak779 or 7.5 µg/ml T20. Cells
475 lysates (20 µg per lane) were prepared with RIPA buffer (25 mM Tris-HCl pH 7.6, 150 mM NaCl,
476 1% NP-40, 1% sodium deoxycholate, 0.1% SDS), containing protease inhibitor cocktail (Sigma)
477 and phosphatase inhibitors (sodium orthovanadate, sodium fluoride and beta-glycerophosphate),
478 and were separated on NuPAGE Bis-Tris gels (ThermoFisher) and transferred onto PVDF
479 membranes. Membranes were probed with mouse anti-SAMHD1 (2D7, Origene, 1:2000), rabbit
480 anti-phT592-SAMHD1 (Cell Signalling Technology, 1:1000) and rabbit anti-GAPDH (Sigma,1:5000)
481 and quantified using the Odyssey far red imager (LiCor).

482

483 Figure Legends

484 Figure 1

485 Human TRIMCyp and TRIM5α inhibit HIV-1 of macrophages but are differentially affected by
486 CypA. (A) The TRIM5 locus of a pluripotent stem cell line was targeted by CRISPR-Cas9 nickase
487 at two sites (black arrow) within exon 8 to initiate homologous recombination with a plasmid
488 donor template containing human CypA (hashed box). TRIM5 was also targeted with wildtype
489 CRISPR-Cas9 targeting exon 2 (grey arrow) to produce a knockout phenotype. (B) Sequence
490 trace of the TRIM5 locus at the insertion site of CypA in the identified double knock-in single
491 cell clone. Infection of stem cells (C) and pMacs (D) from an unmodified clone (TRIM5α) and the
492 genetically modified clone (TRIMCyp) with VSV-G-pseudotyped lentiviral vectors, in the

493 presence of 5 μ M CsA or DMSO, were quantified by flow cytometry for the reporter eGFP
494 protein. Area under the curve (AUC) analysis of the lower 6 values of one representative serial
495 dilution performed twice (C) or lower 4 values of four (D) independent serial dilutions are
496 shown +/- SEM (* p <0.05, *** p <0.001, **** p <0.0001 from a 2-way ANOVA with Turkey's
497 multiple comparisons test. (E) Infection results (mean +/- SEM) for three different vector
498 constructs all pseudotyped with JRFL envelope, normalized to the infectivity of each vector in
499 DMSO treated wildtype pMacs (TRIM5 α) (*** p <0.001, **** p <0.0001, for one-sample t-test to
500 hypothetical value of 100, and * p <0.05 for t test). (F) Infectivity of pMacs to replication
501 competent NL-LucR.T2A measured at day 7 post infection in 3-4 independent experiments,
502 plotted as mean +/- standard deviation (*** p <0.001, **** p <0.0001 for one-sample t-test to
503 hypothetical value of 100). Inset, a representative growth curve performed in quadruplicate
504 over 5 days showing infection as relative light units (RLU) of luciferase. (G) Serial dilutions of
505 VSV-G pseudotyped eGFP-reporter vector or (H) a P90A capsid mutant vector on pMacs from
506 two wildtype clones (TRIM5 α +/+) and two knockout clones (TRIM5 α -/-) in the presence of 5
507 μ M CsA or DMSO. The mean +/- SEM of the infectivity, measured as multiplicity of infection
508 (MOI) at each dilution from three independent experiments are shown.

509

510

511 Figure 2

512 Cell-cell infection of pMacs overcomes TRIMCyp. (A) Macrophages co-cultured with NL-

513 LucR.T2A -infected Jurkat-R5 cells for 6 hours were measured for infection after 7 days, during

514 which etoposide treatment removed residual T cells. Co-cultures were performed in the
515 presence or absence of AZT and are presented as the level of luciferase normalized to the
516 wildtype (TRIM5 α) pMacs in the absence of AZT. Results are plotted as mean +/- standard
517 deviation of 3 independent experiments. (B) Effect of AZT on cell free infection of pMacs
518 measured 7 days post infection. Results are plotted as mean +/- standard deviation of 3
519 independent experiments normalized to the no drug control (*p<0.05, t-test). (C) Effect of anti-
520 HIV drugs AZT and T20 on pMac infection in the cell-cell infection model, co-culturing the cells
521 for 16 hours followed by 4 days etoposide treatment prior to luciferase measurement. Results
522 (raw relative light units or RLU) show the mean +/- standard deviation from three different
523 donor (lines 856-03-04, OX1.19 and HUES2) pMacs (***p<0.001, t-test). (D) Cell-cell infection of
524 pMacs from NL-LucR.T2A infected PBMC-derived CD4+ T cells is enhanced by inhibiting IFN
525 signalling using the JAK1/2 inhibitor Ruxolitinib (Rux). Results are depicted as the mean +/-
526 standard deviation from three different donors normalized to untreated wildtype TRIM5 α -
527 expressing macrophages (*p<0.05, t-test with Holm-Sidak method for correction for multiple
528 comparisons). (E) Results from (D) were normalized to the level of infection of each
529 macrophage population in the presence of AZT (*p<0.05, one-sample t-test to hypothetical
530 value of 100, and **p<0.01, t-test). (F) Supernatants from (D) were assayed by Luminex for a
531 variety of cytokines/chemokines, a subset of which are shown. The results are plotted
532 individually with mean +/- standard deviation indicated (**p<0.01, Kruskal-Wallis test, *p<0.05,
533 ANOVA with Sidak's multiple comparison correction) and the limit of detection is indicated by
534 the hashed area. (G) Representative micrographs of wildtype macrophages on day 7 post co-
535 culture with donor derived infected T cells, with black arrows depicting giant syncytial cells.

536 Figure 3

537 Heterocytium formation results in reverse-transcriptase independent macrophage infection. (A)
538 Representative images of two HIV-1 eGFP-reporter virus infected Jurkat-R5 cells (green) fusing
539 with stem cell-derived macrophages (red). (B) Quantification of cell fates of infected Jurkat-R5 T
540 cells within the co-culture over a 2-hour period. The average number of events from 4 fields of
541 view is also shown. (C) SAMHD1-knockout macrophages show elevated levels and kinetics of
542 infection. The replication of NL-LucR.T2A virus in SAMHD1-knockout macrophages from three
543 independent pMac factories performed in triplicate is shown as mean +/- standard deviation
544 and is compared to that of the parental isogenic wildtype (WT) macrophages. (D) Co-culture of
545 NL-LucR.T2A infected Jurkat-R5 cells with an isogenic pair of macrophages, differing only in the
546 loss of SAMHD1, shows that restriction by SAMHD1 is overcome by cell fusion. Infectivity of the
547 macrophages, in the presence or absence of AZT and T20, was measured 5 days post co-culture
548 with 4 days of etoposide treatment. Results (raw RLU values) are presented as the mean +/-
549 standard deviation of three independent co-culture experiments. (E) Ratio of phosphorylated to
550 total SAMHD1 levels within the co-culture of pMacs and HIV-1 envelope-expressing CEM T cells.
551 The mean +/- standard deviation of 3-5 experiments using two pMac donors are shown, with
552 fusion being prevented by the inhibitors T20 or Tak779, or by use of CEM cells lacking the HIV-1
553 envelope (**p<0.01, t-test). (F) HIV-1 eGFP-reporter virus infected Jurkat-R5 cells (green),
554 cultured with tRFP-expressing microglial precursors (pMGL, red), both stained with Hoechst
555 33342 to identify nuclei (blue), form heterocytia with classical giant cell morphology (white
556 arrows) compared with macrophage heterocytia (pMac), in the presence of AZT but not T20.

557 Supplemental Fig 1

558 Endogenous expression of TRIMCyp is restrictive to HIV-1 in pluripotent stem cells. Serial
559 dilutions of a VSV-G pseudotyped lentiviral vector were used to infect pluripotent stem cells of
560 the wildtype clone (TRIM5 α) and the genetically modified line (TRIMCyp). The multiplicity of
561 infection (MOI) at different dilutions of virus, as measured by flow cytometry for the reporter
562 gene eGFP, are shown as the mean +/- standard deviation of a representative experiment
563 performed in triplicate. (A-E) depict different combinations of cell types and treatments (CsA at
564 5 μ M) for clarity, all of which is summarized in Fig. 1C. (F) Schematic representation of the
565 interplay between HIV-1 core (image adapted from (76)), the PRYSPRY domain of TRIM5 α (red),
566 the Cyp domain of TRIMCyp (blue) and the host cyclophilin A (blue ovals) in the presence and
567 absence of cyclosporin A (CsA).

568 Supplemental Fig 2

569 Endogenous expression of TRIMCyp is restrictive to HIV-1 in stem cell-derived macrophages.
570 Serial dilutions of a VSV-G-pseudotyped eGFP-expressing lentiviral vector were used to infect
571 pMacs derived from the wildtype stem cell clone (TRIM5 α) and the genetically modified line
572 (TRIMCyp). The multiplicity of infection (MOI) at different dilutions of virus, as measured by
573 flow cytometry for the reporter gene eGFP, are shown as the mean +/- standard deviation of
574 four independent experiments. (A-E) depict different combinations of cell types and treatments
575 (CsA at 5 μ M) for clarity, all of which is summerised in Fig. 1D.

576

577 Supplemental Fig 3

578 Cell-cell interactions in co-cultures of pMacs and HIV-1 infected T cells. Jurkat-R5 cells, infected
579 with a replication-competent eGFP-reporter virus, were co-cultured with CellTracker Red
580 labeled pMacs and imaged over time. Representative images are shown depicting (A) cell
581 capture (phagocytosis), (B) apoptosis followed by phagocytosis, (C) GFP loss (cell lysis), (D) viral
582 transfer (highlighted with white arrow). (E) Effect of fusion on SAMHD1 phosphorylation. A
583 representative western blot shows the level of total (SAMHD1) and T592-phosphorylated (P-
584 SAMHD1) SAMHD1 as well as the loading control (GAPDH). Macrophages alone (pMac only),
585 CEM T cells alone (CEM only), and co-cultured cells incapable of fusing either through lack of
586 HIV-1 envelope (pMac+CEM) or addition of a fusion inhibitor (pMac+CEMH0-BaL+Tak779) were
587 compared to co-cultures allowed to fuse (pMac+CEMH0-BaL).

588 Supplemental Fig 4

589 Quality control of the TRIMCyp stem cells and pMacs. (A) SNP analysis (OmniExpress24 chip) of
590 the parental line, wildtype clone (TRIM5 α) and modified line (TRIMCyp) are shown, analysed
591 using KaryoStudio (Illumina) to detect copy number variations across the genomes. Duplications
592 are shown in green, deletions in red and loss of heterozygosity in grey. (B) Flow cytometry
593 analysis of antibody staining for key pluripotent stem cell markers, TRA-1-60 and NANOG (dark
594 grey), on the stem cell clones of wildtype and genetically modified cell lines versus their
595 respective isotype controls (light grey). Stem cells were fixed in 2% paraformaldehyde, followed
596 by re-suspension in ice-cold 100% methanol before washing in FACS buffer (PBS with 10 μ g/ml
597 IgG from human serum, and 2.5% FBS). Antibodies used included anti-Tra-1-60-Alexa⁴⁸⁸
598 (Biolegend), anti-NANOG-Alexa⁶⁴⁷ (Cell Signaling) and isotope control antibodies IgM-Alexa⁴⁸⁸
599 (Biolegend) and IgG-Alexa⁶⁴⁷ (Cell Signaling). (C) Flow cytometry analysis of antibody staining

600 (dark grey) for the myeloid specific lineage marker CD14 and CD68, versus their isotype controls
601 (light grey) on pMacs differentiated from the wildtype and modified cell lines. Antibodies used
602 included anti-CD14-FITC, anti CD68-FITC and their respective isotype controls (all from
603 Immunotools).

604 Supplemental Video 1

605 Macrophage infection through cell-cell fusion. HIV-1 eGFP-reporter virus infected Jurkat-R5 cells
606 (green) were cultured with CellTracker Red labelled stem cell-derived macrophages (red), in the
607 presence of Hoechst 33342 to identify nuclei and imaged every 5 minutes. The video shown is a
608 representative video of those used to generate data for Fig 3A+B+S3. Multiple fusion events
609 can be observed as eGFP expressed from the T cells is rapidly transferred to the macrophages.

610

611 Acknowledgments

612 This publication arises from research funded by the John Fell Oxford University Press (OUP)
613 Research Fund. The pluripotent stem cell lines used in this study were originally generated from
614 donor samples supplied by the Oxford Parkinson's Disease Centre (OPDC) study (funded by the
615 Monument Trust Discovery Award from Parkinson's UK, a charity registered in England and
616 Wales (2581970) and in Scotland (SC037554), with the support of the National Institute for
617 Health Research (NIHR) Oxford Biomedical Research Centre based at Oxford University
618 Hospitals NHS Trust and University of Oxford, and the NIHR Comprehensive Local Research
619 Network), and was reprogrammed within StemBANCC, (supported by the Innovative Medicines
620 Initiative Joint Undertaking under grant agreement number 115439, resources of which are

621 composed of financial contribution from the European Union's Seventh Framework Program
622 (FP7/2007e2013) and EFPIA companies' in kind contribution). AV-J and LN are supported by the
623 Infection, Immunology and Translation Medicine Wellcome Trust-funded DTC (grant numbers
624 203805/Z/16/Z and 108869/Z/15/Z, respectively). The funders had no role in study design, data
625 collection and interpretation, or the decision to submit the work for publication.

626

627 Conflict of interest

628 The authors declare that they have no conflicts of interest with the contents of this article.

629

630 Author Contributions

631 MDM designed, carried out, experiments, analysed data and prepared the manuscript. HO, AV-
632 J, LN, JV carried out experiments. WJ and AVJ analysed data and prepared the manuscript.

633

634

635

636 References

- 637 1. **Gordon S, Pluddemann A.** 2017. Tissue macrophages: heterogeneity and functions. *BMC Biol*
638 **15**:53.
- 639 2. **Hoeffel G, Ginhoux F.** 2015. Ontogeny of Tissue-Resident Macrophages. *Front Immunol* **6**:486.
- 640 3. **Stremlau M, Owens CM, Perron MJ, Kiessling M, Autissier P, Sodroski J.** 2004. The cytoplasmic
641 body component TRIM5 α restricts HIV-1 infection in Old World monkeys. *Nature* **427**:848-
642 853.

- 643 4. **Luban J.** 2012. TRIM5 and the Regulation of HIV-1 Infectivity. *Mol Biol Int* **2012**:426840.
- 644 5. **Stremlau M, Perron M, Welikala S, Sodroski J.** 2005. Species-specific variation in the
645 B30.2(SPRY) domain of TRIM5alpha determines the potency of human immunodeficiency virus
646 restriction. *J Virol* **79**:3139-3145.
- 647 6. **Wu F, Kirmaier A, Goeken R, Ourmanov I, Hall L, Morgan JS, Matsuda K, Buckler-White A,**
648 **Tomioka K, Plishka R, Whitted S, Johnson W, Hirsch VM.** 2013. TRIM5 alpha drives SIVsmm
649 evolution in rhesus macaques. *PLoS Pathog* **9**:e1003577.
- 650 7. **Yap MW, Nisole S, Stoye JP.** 2005. A single amino acid change in the SPRY domain of human
651 Trim5alpha leads to HIV-1 restriction. *Curr Biol* **15**:73-78.
- 652 8. **Keckesova Z, Ylinen LM, Towers GJ.** 2006. Cyclophilin A renders human immunodeficiency virus
653 type 1 sensitive to Old World monkey but not human TRIM5 alpha antiviral activity. *J Virol*
654 **80**:4683-4690.
- 655 9. **Rasaiyaah J, Tan CP, Fletcher AJ, Price AJ, Blondeau C, Hilditch L, Jacques DA, Selwood DL,**
656 **James LC, Noursadeghi M, Towers GJ.** 2013. HIV-1 evades innate immune recognition through
657 specific cofactor recruitment. *Nature* **503**:402-405.
- 658 10. **Virgen CA, Kratovac Z, Bieniasz PD, Hatziioannou T.** 2008. Independent genesis of chimeric
659 TRIM5-cyclophilin proteins in two primate species. *Proc Natl Acad Sci U S A* **105**:3563-3568.
- 660 11. **Wilson SJ, Webb BL, Ylinen LM, Verschoor E, Heeney JL, Towers GJ.** 2008. Independent
661 evolution of an antiviral TRIMCyp in rhesus macaques. *Proc Natl Acad Sci U S A* **105**:3557-3562.
- 662 12. **Kirmaier A, Wu F, Newman RM, Hall LR, Morgan JS, O'Connor S, Marx PA, Meythaler M,**
663 **Goldstein S, Buckler-White A, Kaur A, Hirsch VM, Johnson WE.** 2010. TRIM5 suppresses cross-
664 species transmission of a primate immunodeficiency virus and selects for emergence of resistant
665 variants in the new species. *PLoS Biol* **8**.
- 666 13. **Nakayama EE, Shioda T.** 2012. TRIM5alpha and Species Tropism of HIV/SIV. *Front Microbiol*
667 **3**:13.
- 668 14. **Chan E, Schaller T, Eddaoudi A, Zhan H, Tan CP, Jacobsen M, Thrasher AJ, Towers GJ, Qasim W.**
669 2012. Lentiviral gene therapy against human immunodeficiency virus type 1, using a novel
670 human TRIM21-cyclophilin A restriction factor. *Hum Gene Ther* **23**:1176-1185.
- 671 15. **Chan E, Towers GJ, Qasim W.** 2014. Gene therapy strategies to exploit TRIM derived restriction
672 factors against HIV-1. *Viruses* **6**:243-263.
- 673 16. **Pertel T, Hausmann S, Morger D, Zuger S, Guerra J, Lascano J, Reinhard C, Santoni FA, Uchil PD,**
674 **Chatel L, Bisiaux A, Albert ML, Strambio-De-Castillia C, Mothes W, Pizzato M, Grutter MG,**
675 **Luban J.** 2011. TRIM5 is an innate immune sensor for the retrovirus capsid lattice. *Nature*
676 **472**:361-365.
- 677 17. **Goldstone DC, Ennis-Adeniran V, Hedden JJ, Groom HC, Rice GI, Christodoulou E, Walker PA,**
678 **Kelly G, Haire LF, Yap MW, de Carvalho LP, Stoye JP, Crow YJ, Taylor IA, Webb M.** 2011. HIV-1
679 restriction factor SAMHD1 is a deoxynucleoside triphosphate triphosphohydrolase. *Nature*
680 **480**:379-382.
- 681 18. **Franzolin E, Pontarin G, Rampazzo C, Miazzi C, Ferraro P, Palumbo E, Reichard P, Bianchi V.**
682 2013. The deoxynucleotide triphosphohydrolase SAMHD1 is a major regulator of DNA precursor
683 pools in mammalian cells. *Proc Natl Acad Sci U S A* **110**:14272-14277.
- 684 19. **Lahouassa H, Daddacha W, Hofmann H, Ayinde D, Logue EC, Dragin L, Bloch N, Maudet C,**
685 **Bertrand M, Gramberg T, Pancino G, Priet S, Canard B, Laguet N, Benkirane M, Transy C,**
686 **Landau NR, Kim B, Margottin-Goguet F.** 2012. SAMHD1 restricts the replication of human
687 immunodeficiency virus type 1 by depleting the intracellular pool of deoxynucleoside
688 triphosphates. *Nat Immunol* **13**:223-228.

- 689 20. **Mock DJ, Hollenbaugh JA, Daddacha W, Overstreet MG, Lazarski CA, Fowell DJ, Kim B.** 2012.
690 Leishmania induces survival, proliferation and elevated cellular dNTP levels in human monocytes
691 promoting acceleration of HIV co-infection. *PLoS Pathog* **8**:e1002635.
- 692 21. **Schmidt S, Schenkova K, Adam T, Erikson E, Lehmann-Koch J, Sertel S, Verhasselt B, Fackler OT,**
693 **Lasitschka F, Keppler OT.** 2015. SAMHD1's protein expression profile in humans. *J Leukoc Biol*
694 **98**:5-14.
- 695 22. **de Silva S, Hoy H, Hake TS, Wong HK, Porcu P, Wu L.** 2013. Promoter methylation regulates
696 SAMHD1 gene expression in human CD4+ T cells. *J Biol Chem* **288**:9284-9292.
- 697 23. **Ruffin N, Brezar V, Ayinde D, Lefebvre C, Schulze Zur Wiesch J, van Lunzen J, Bockhorn M,**
698 **Schwartz O, Hocini H, Lelievre JD, Banchereau J, Levy Y, Seddiki N.** 2015. Low SAMHD1
699 expression following T-cell activation and proliferation renders CD4+ T cells susceptible to HIV-1.
700 *AIDS* **29**:519-530.
- 701 24. **Laguet N, Sobhian B, Casartelli N, Ringeard M, Chable-Bessia C, Segeral E, Yatim A, Emiliani**
702 **S, Schwartz O, Benkirane M.** 2011. SAMHD1 is the dendritic- and myeloid-cell-specific HIV-1
703 restriction factor counteracted by Vpx. *Nature* **474**:654-657.
- 704 25. **Buchrieser J, James W, Moore MD.** 2017. Human Induced Pluripotent Stem Cell-Derived
705 Macrophages Share Ontogeny with MYB-Independent Tissue-Resident Macrophages. *Stem Cell*
706 *Reports* **8**:334-345.
- 707 26. **Haenseler W, Sansom SN, Buchrieser J, Newey SE, Moore CS, Nicholls FJ, Chintawar S, Schnell**
708 **C, Antel JP, Allen ND, Cader MZ, Wade-Martins R, James WS, Cowley SA.** 2017. A Highly
709 Efficient Human Pluripotent Stem Cell Microglia Model Displays a Neuronal-Co-culture-Specific
710 Expression Profile and Inflammatory Response. *Stem Cell Reports* **8**:1727-1742.
- 711 27. **Ran FA, Hsu PD, Lin CY, Gootenberg JS, Konermann S, Trevino AE, Scott DA, Inoue A, Matoba S,**
712 **Zhang Y, Zhang F.** 2013. Double nicking by RNA-guided CRISPR Cas9 for enhanced genome
713 editing specificity. *Cell* **154**:1380-1389.
- 714 28. **Neagu MR, Ziegler P, Pertel T, Strambio-De-Castillia C, Grutter C, Martinetti G, Mazzucchelli L,**
715 **Grutter M, Manz MG, Luban J.** 2009. Potent inhibition of HIV-1 by TRIM5-cyclophilin fusion
716 proteins engineered from human components. *J Clin Invest* **119**:3035-3047.
- 717 29. **van Wilgenburg B, Browne C, Vowles J, Cowley SA.** 2013. Efficient, long term production of
718 monocyte-derived macrophages from human pluripotent stem cells under partly-defined and
719 fully-defined conditions. *PLoS One* **8**:e71098.
- 720 30. **Rowe HM, Kapopoulou A, Corsinotti A, Fasching L, Macfarlan TS, Tarabay Y, Viville S,**
721 **Jakobsson J, Pfaff SL, Trono D.** 2013. TRIM28 repression of retrotransposon-based enhancers is
722 necessary to preserve transcriptional dynamics in embryonic stem cells. *Genome Res* **23**:452-
723 461.
- 724 31. **Shi J, Aiken C.** 2006. Saturation of TRIM5 alpha-mediated restriction of HIV-1 infection depends
725 on the stability of the incoming viral capsid. *Virology* **350**:493-500.
- 726 32. **Hatzioannou T, Perez-Caballero D, Yang A, Cowan S, Bieniasz PD.** 2004. Retrovirus resistance
727 factors Ref1 and Lv1 are species-specific variants of TRIM5alpha. *Proc Natl Acad Sci U S A*
728 **101**:10774-10779.
- 729 33. **Ribeiro CM, Sarrami-Forooshani R, Setiawan LC, Zijlstra-Willems EM, van Hamme JL,**
730 **Tigchelaar W, van der Wel NN, Kootstra NA, Gringhuis SI, Geijtenbeek TB.** 2016. Receptor
731 usage dictates HIV-1 restriction by human TRIM5alpha in dendritic cell subsets. *Nature* **540**:448-
732 452.
- 733 34. **D'Angelo W, Gurung C, Acharya D, Chen B, Ortolano N, Gama V, Bai F, Guo YL.** 2017. The
734 Molecular Basis for the Lack of Inflammatory Responses in Mouse Embryonic Stem Cells and
735 Their Differentiated Cells. *J Immunol* **198**:2147-2155.

- 736 35. **Pushkarsky T, Zybarth G, Dubrovsky L, Yurchenko V, Tang H, Guo H, Toole B, Sherry B,**
737 **Bukrinsky M.** 2001. CD147 facilitates HIV-1 infection by interacting with virus-associated
738 cyclophilin A. *Proc Natl Acad Sci U S A* **98**:6360-6365.
- 739 36. **Duncan CJ, Russell RA, Sattentau QJ.** 2013. High multiplicity HIV-1 cell-to-cell transmission from
740 macrophages to CD4+ T cells limits antiretroviral efficacy. *Aids* **27**:2201-2206.
- 741 37. **Russell RA, Martin N, Mitar I, Jones E, Sattentau QJ.** 2013. Multiple proviral integration events
742 after virological synapse-mediated HIV-1 spread. *Virology* **443**:143-149.
- 743 38. **Baxter AE, Russell RA, Duncan CJ, Moore MD, Willberg CB, Pablos JL, Finzi A, Kaufmann DE,**
744 **Ochsenbauer C, Kappes JC, Groot F, Sattentau QJ.** 2014. Macrophage infection via selective
745 capture of HIV-1-infected CD4+ T cells. *Cell Host Microbe* **16**:711-721.
- 746 39. **Lalezari JP, Eron JJ, Carlson M, Cohen C, DeJesus E, Arduino RC, Gallant JE, Volberding P,**
747 **Murphy RL, Valentine F, Nelson EL, Sista PR, Dusek A, Kilby JM.** 2003. A phase II clinical study of
748 the long-term safety and antiviral activity of enfuvirtide-based antiretroviral therapy. *AIDS*
749 **17**:691-698.
- 750 40. **Dargent JL, Lespagnard L, Kornreich A, Hermans P, Clumeck N, Verhest A.** 2000. HIV-associated
751 multinucleated giant cells in lymphoid tissue of the Waldeyer's ring: a detailed study. *Mod*
752 *Pathol* **13**:1293-1299.
- 753 41. **Harbison C, Zhuang K, Gettie A, Blanchard J, Knight H, Didier P, Cheng-Mayer C, Westmoreland**
754 **S.** 2014. Giant cell encephalitis and microglial infection with mucosally transmitted simian-
755 human immunodeficiency virus SHIVSF162P3N in rhesus macaques. *J Neurovirol* **20**:62-72.
- 756 42. **Gary R, Voelkl S, Palmisano R, Ullrich E, Bosch JJ, Mackensen A.** 2012. Antigen-specific transfer
757 of functional programmed death ligand 1 from human APCs onto CD8+ T cells via trogocytosis. *J*
758 *Immunol* **188**:744-752.
- 759 43. **Jolly C, Kashefi K, Hollinshead M, Sattentau QJ.** 2004. HIV-1 cell to cell transfer across an Env-
760 induced, actin-dependent synapse. *J Exp Med* **199**:283-293.
- 761 44. **Wills QF, Mellado-Gomez E, Nolan R, Warner D, Sharma E, Broxholme J, Wright B, Lockstone**
762 **H, James W, Lynch M, Gonzales M, West J, Leyrat A, Padilla-Parra S, Filippi S, Holmes C, Moore**
763 **MD, Bowden R.** 2017. The nature and nurture of cell heterogeneity: accounting for macrophage
764 gene-environment interactions with single-cell RNA-Seq. *BMC Genomics* **18**:53.
- 765 45. **Avalos CR, Abreu CM, Queen SE, Li M, Price S, Shirk EN, Engle EL, Forsyth E, Bullock BT, Mac**
766 **Gabhann F, Wietgreffe SW, Haase AT, Zink MC, Mankowski JL, Clements JE, Gama L.** 2017. Brain
767 Macrophages in Simian Immunodeficiency Virus-Infected, Antiretroviral-Suppressed Macaques:
768 a Functional Latent Reservoir. *MBio* **8**.
- 769 46. **Deeks SG, Barre-Sinoussi F.** 2012. Public health: Towards a cure for HIV. *Nature* **487**:293-294.
- 770 47. **Mlcochova P, Sutherland KA, Watters SA, Bertoli C, de Bruin RA, Rehwinkel J, Neil SJ, Lenzi**
771 **GM, Kim B, Khwaja A, Gage MC, Georgiou C, Chittka A, Yona S, Noursadeghi M, Towers GJ,**
772 **Gupta RK.** 2017. A G1-like state allows HIV-1 to bypass SAMHD1 restriction in macrophages.
773 *Embo j* **36**:604-616.
- 774 48. **Towers GJ, Hatziioannou T, Cowan S, Goff SP, Luban J, Bieniasz PD.** 2003. Cyclophilin A
775 modulates the sensitivity of HIV-1 to host restriction factors. *Nat Med* **9**:1138-1143.
- 776 49. **Kellam P, Larder BA.** 1995. Retroviral recombination can lead to linkage of reverse transcriptase
777 mutations that confer increased zidovudine resistance. *J Virol* **69**:669-674.
- 778 50. **Luban J.** 2007. Cyclophilin A, TRIM5, and resistance to human immunodeficiency virus type 1
779 infection. *J Virol* **81**:1054-1061.
- 780 51. **Sokolskaja E, Berthoux L, Luban J.** 2006. Cyclophilin A and TRIM5alpha independently regulate
781 human immunodeficiency virus type 1 infectivity in human cells. *J Virol* **80**:2855-2862.
- 782 52. **Schaller T, Ocwieja KE, Rasaiyaah J, Price AJ, Brady TL, Roth SL, Hue S, Fletcher AJ, Lee K,**
783 **KewalRamani VN, Noursadeghi M, Jenner RG, James LC, Bushman FD, Towers GJ.** 2011. HIV-1

- 784 capsid-cyclophilin interactions determine nuclear import pathway, integration targeting and
785 replication efficiency. *PLoS Pathog* **7**:e1002439.
- 786 53. **Campbell EM, Weingart J, Sette P, Opp S, Sastri J, O'Connor SK, Talley S, Diaz-Griffero F, Hirsch**
787 **V, Bouamr F.** 2016. TRIM5alpha-Mediated Ubiquitin Chain Conjugation Is Required for Inhibition
788 of HIV-1 Reverse Transcription and Capsid Destabilization. *J Virol* **90**:1849-1857.
- 789 54. **Billich A, Hammerschmid F, Peichl P, Wenger R, Zenke G, Quesniaux V, Rosenwirth B.** 1995.
790 Mode of action of SDZ NIM 811, a nonimmunosuppressive cyclosporin A analog with activity
791 against human immunodeficiency virus (HIV) type 1: interference with HIV protein-cyclophilin A
792 interactions. *J Virol* **69**:2451-2461.
- 793 55. **Ptak RG, Gallay PA, Jochmans D, Halestrap AP, Rugg UT, Pallansch LA, Bobardt MD, de**
794 **Bethune MP, Neyts J, De Clercq E, Dumont JM, Scalfaro P, Besseghir K, Wenger RM,**
795 **Rosenwirth B.** 2008. Inhibition of human immunodeficiency virus type 1 replication in human
796 cells by Debio-025, a novel cyclophilin binding agent. *Antimicrob Agents Chemother* **52**:1302-
797 1317.
- 798 56. **Flisiak R, Horban A, Gallay P, Bobardt M, Selvarajah S, Wiercinska-Drapalo A, Siwak E, Cielniak**
799 **I, Higersberger J, Kierkus J, Aeschlimann C, Groscurin P, Nicolas-Metral V, Dumont JM, Porchet**
800 **H, Crabbe R, Scalfaro P.** 2008. The cyclophilin inhibitor Debio-025 shows potent anti-hepatitis C
801 effect in patients coinfecting with hepatitis C and human immunodeficiency virus. *Hepatology*
802 **47**:817-826.
- 803 57. **Rizzardì GP, Harari A, Capiluppi B, Tambussi G, Ellefsen K, Ciuffreda D, Champagne P, Bart PA,**
804 **Chave JP, Lazzarin A, Pantaleo G.** 2002. Treatment of primary HIV-1 infection with cyclosporin A
805 coupled with highly active antiretroviral therapy. *J Clin Invest* **109**:681-688.
- 806 58. **Markowitz M, Vaida F, Hare CB, Boden D, Mohri H, Hecht FM, Kalayjian RC, Conrad A, Mildvan**
807 **D, Aberg J, Hogan C, Kilby JM, Balfour HH, Jr., Schafer K, Richman D, Little S.** 2010. The virologic
808 and immunologic effects of cyclosporine as an adjunct to antiretroviral therapy in patients
809 treated during acute and early HIV-1 infection. *J Infect Dis* **201**:1298-1302.
- 810 59. **Okafo G, Prevedel L, Eugenin E.** 2017. Tunneling nanotubes (TNT) mediate long-range gap
811 junctional communication: Implications for HIV cell to cell spread. *Sci Rep* **7**:16660.
- 812 60. **Fouchier RA, Meyaard L, Brouwer M, Hovenkamp E, Schuitemaker H.** 1996. Broader tropism
813 and higher cytopathicity for CD4+ T cells of a syncytium-inducing compared to a non-syncytium-
814 inducing HIV-1 isolate as a mechanism for accelerated CD4+ T cell decline in vivo. *Virology*
815 **219**:87-95.
- 816 61. **Pope M.** 1999. Mucosal dendritic cells and immunodeficiency viruses. *J Infect Dis* **179 Suppl**
817 **3**:S427-430.
- 818 62. **Kolson DL, Gonzalez-Scarano F.** 2000. HIV and HIV dementia. *J Clin Invest* **106**:11-13.
- 819 63. **Symeonides M, Murooka TT, Belfly LN, Roy NH, Mempel TR, Thali M.** 2015. HIV-1-Induced
820 Small T Cell Syncytia Can Transfer Virus Particles to Target Cells through Transient Contacts.
821 *Viruses* **7**:6590-6603.
- 822 64. **Bracq L, Xie M, Lambele M, Vu LT, Matz J, Schmitt A, Delon J, Zhou P, Randriamampita C,**
823 **Bouchet J, Benichou S.** 2017. T cell-macrophage fusion triggers multinucleated giant cell
824 formation for HIV-1 spreading. *J Virol* doi:10.1128/jvi.01237-17.
- 825 65. **Martinez-Mendez D, Rivera-Toledo E, Ortega E, Licona-Limon I, Huerta L.** 2017. Monocyte-
826 lymphocyte fusion induced by the HIV-1 envelope generates functional heterokaryons with an
827 activated monocyte-like phenotype. *Exp Cell Res* **352**:9-19.
- 828 66. **Negi N, Das BK.** 2017. CNS: Not an immunoprivileged site anymore but a virtual secondary
829 lymphoid organ. *Int Rev Immunol* doi:10.1080/08830185.2017.1357719:1-12.
- 830 67. **Calantone N, Wu F, Klase Z, Deleage C, Perkins M, Matsuda K, Thompson EA, Ortiz AM, Vinton**
831 **CL, Ourmanov I, Lore K, Douek DC, Estes JD, Hirsch VM, Brenchley JM.** 2014. Tissue myeloid

- 832 cells in SIV-infected primates acquire viral DNA through phagocytosis of infected T cells.
833 *Immunity* **41**:493-502.
- 834 68. **Cong L, Ran FA, Cox D, Lin S, Barretto R, Habib N, Hsu PD, Wu X, Jiang W, Marraffini LA, Zhang**
835 **F.** 2013. Multiplex genome engineering using CRISPR/Cas systems. *Science* **339**:819-823.
- 836 69. **Flynn R, Grundmann A, Renz P, Hanseler W, James WS, Cowley SA, Moore MD.** 2015. CRISPR-
837 mediated genotypic and phenotypic correction of a chronic granulomatous disease mutation in
838 human iPS cells. *Exp Hematol* **43**:838-848 e833.
- 839 70. **Sanjana NE, Shalem O, Zhang F.** 2014. Improved vectors and genome-wide libraries for CRISPR
840 screening. *Nat Methods* **11**:783-784.
- 841 71. **Brinkman EK, Chen T, Amendola M, van Steensel B.** 2014. Easy quantitative assessment of
842 genome editing by sequence trace decomposition. *Nucleic Acids Res* **42**:e168.
- 843 72. **Rhodes T, Wargo H, Hu WS.** 2003. High rates of human immunodeficiency virus type 1
844 recombination: near-random segregation of markers one kilobase apart in one round of viral
845 replication. *J Virol* **77**:11193-11200.
- 846 73. **He J, Choe S, Walker R, Di Marzio P, Morgan DO, Landau NR.** 1995. Human immunodeficiency
847 virus type 1 viral protein R (Vpr) arrests cells in the G2 phase of the cell cycle by inhibiting
848 p34cdc2 activity. *J Virol* **69**:6705-6711.
- 849 74. **Edmonds TG, Ding H, Yuan X, Wei Q, Smith KS, Conway JA, Wieczorek L, Brown B, Polonis V,**
850 **West JT, Montefiori DC, Kappes JC, Ochsenbauer C.** 2010. Replication competent molecular
851 clones of HIV-1 expressing Renilla luciferase facilitate the analysis of antibody inhibition in
852 PBMC. *Virology* **408**:1-13.
- 853 75. **Levy DN, Aldrovandi GM, Kutsch O, Shaw GM.** 2004. Dynamics of HIV-1 recombination in its
854 natural target cells. *Proc Natl Acad Sci U S A* **101**:4204-4209.
- 855 76. **Pornillos O, Ganser-Pornillos BK, Yeager M.** 2011. Atomic-level modelling of the HIV capsid.
856 *Nature* **469**:424-427.

857

Figure 1

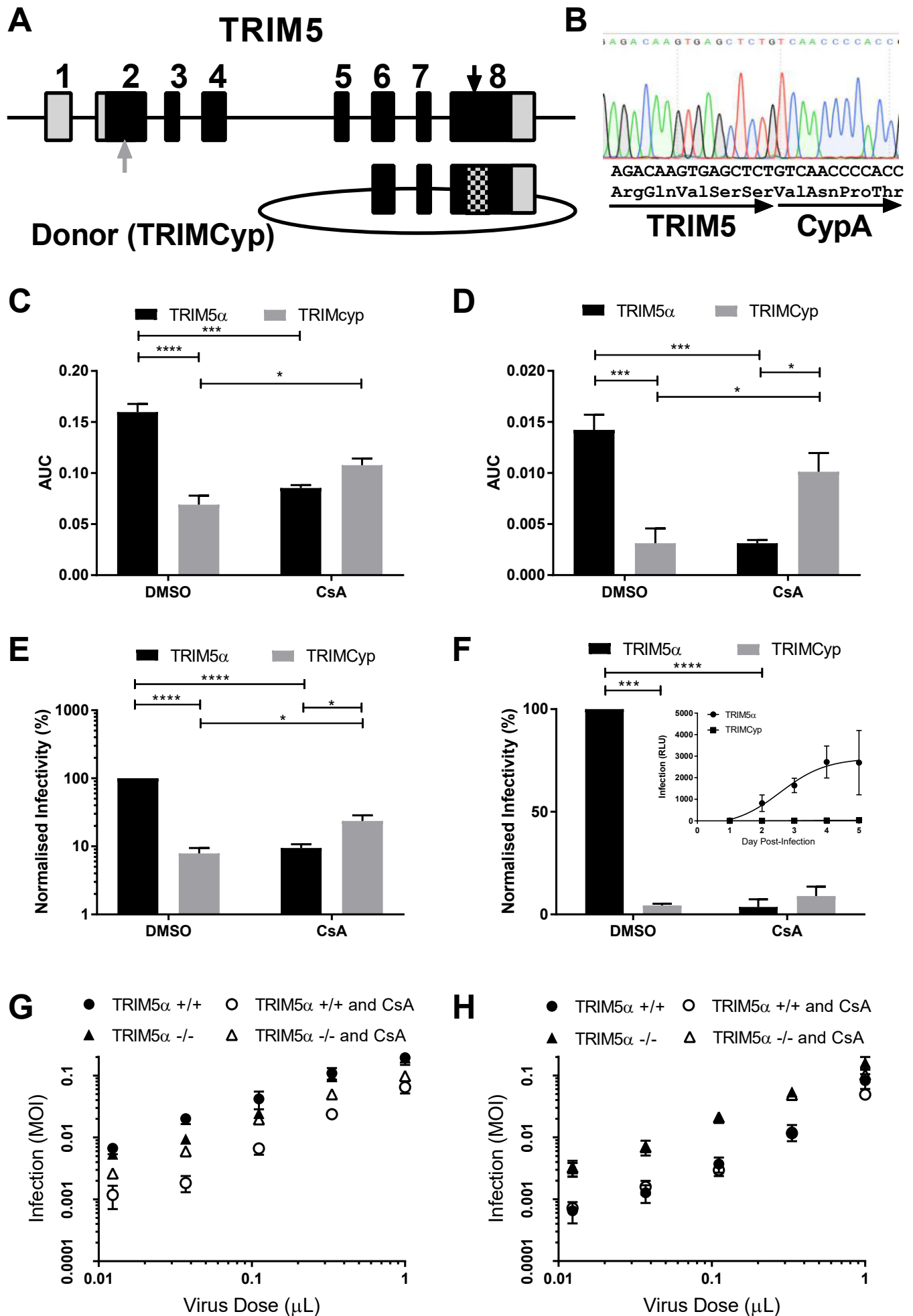


Figure 2

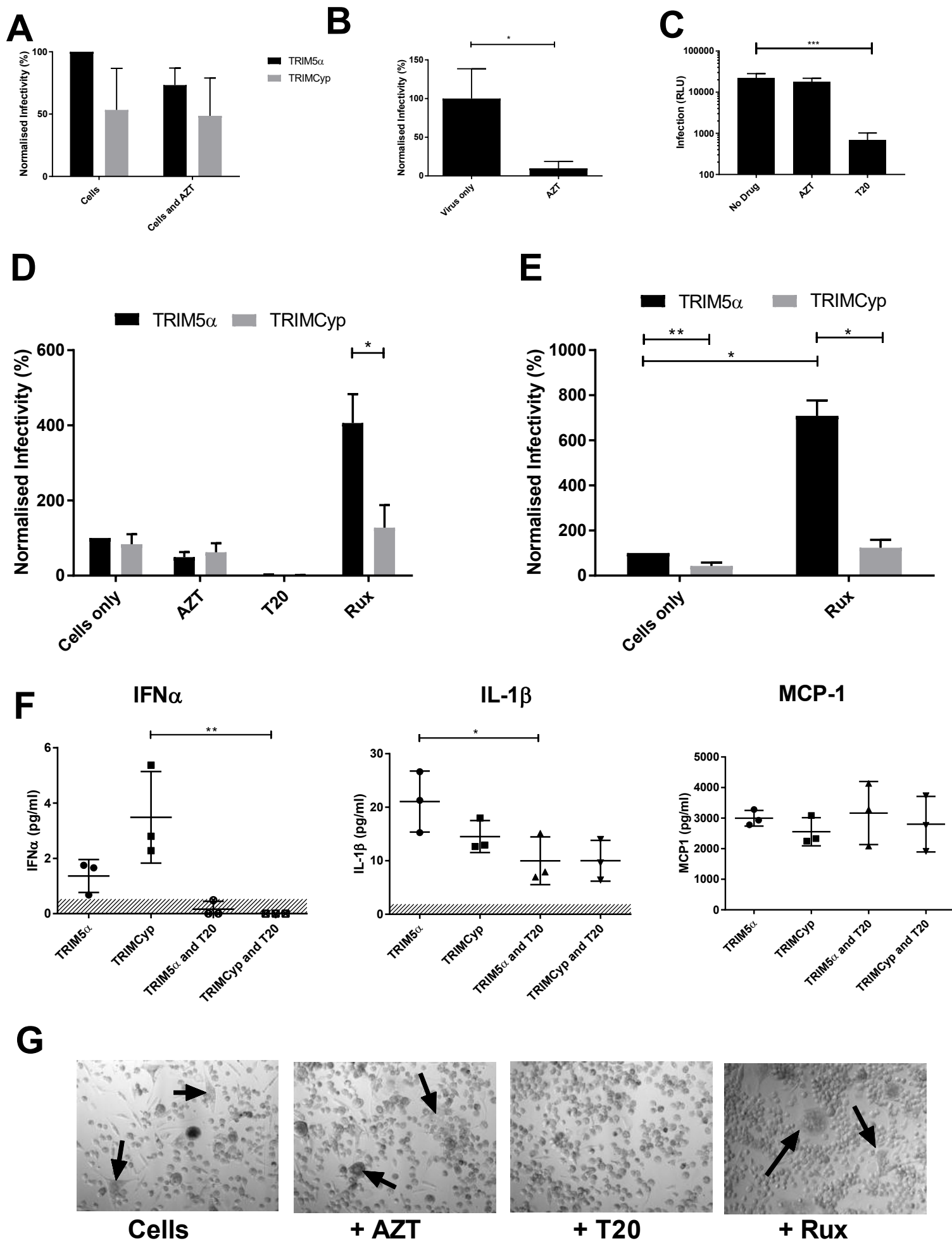
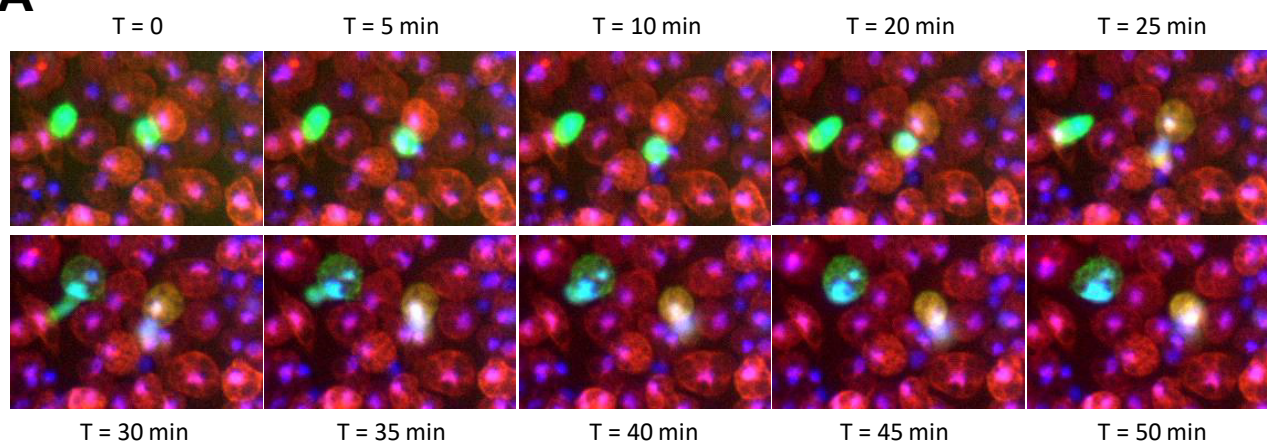
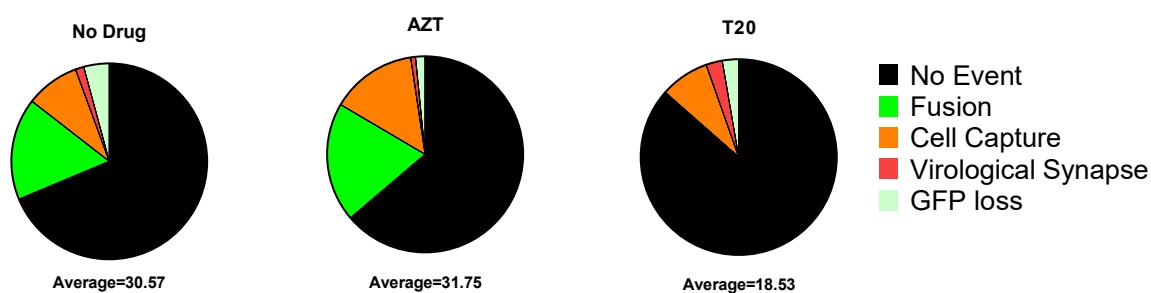


Figure 3

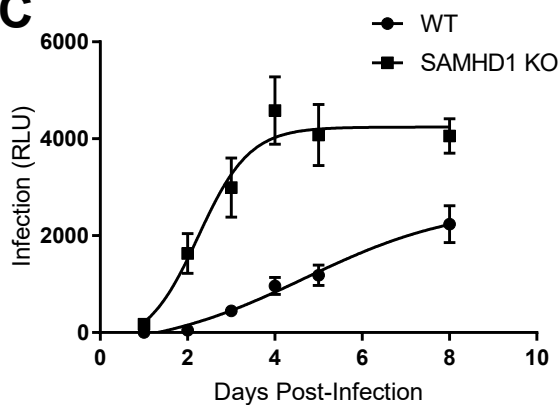
A



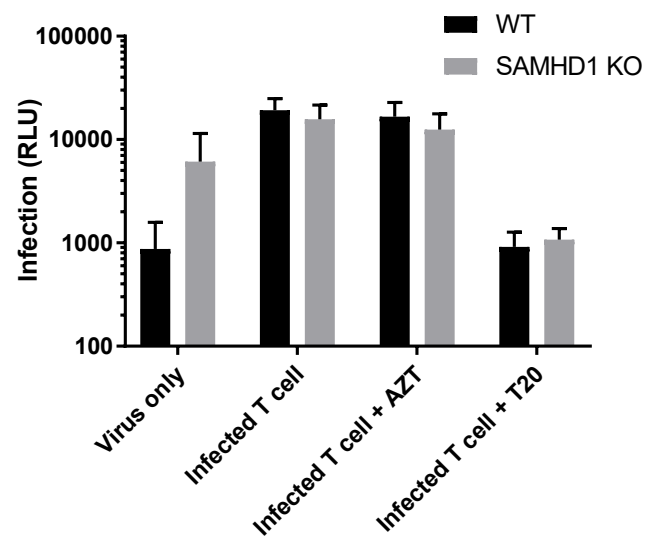
B



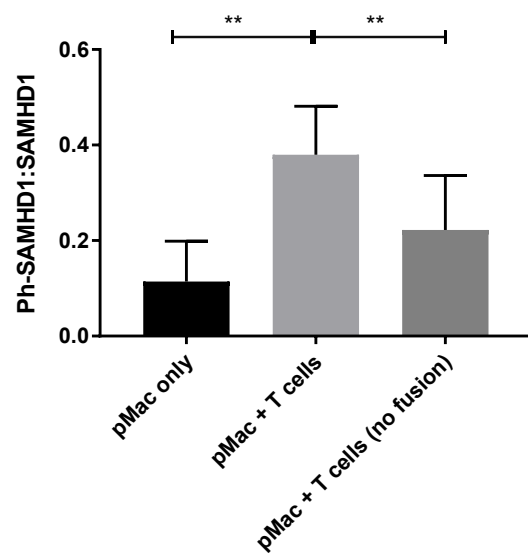
C



D



E



F

